

Abnormal Functional Organization in the Dorsal Lateral Geniculate Nucleus of Mice Lacking the $\beta 2$ Subunit of the Nicotinic Acetylcholine Receptor

Matthew S. Grubb,^{1,3} Francesco M. Rossi,^{2,3,4}
Jean-Pierre Changeux,² and Ian D. Thompson^{1,*}

¹University Laboratory of Physiology
Parks Road
Oxford OX1 3PT
United Kingdom

²Institut Pasteur CNRS URA 2182
"Récepteurs et Cognition"

Departement des Biotechnologies
Institut Pasteur
25 Rue du Docteur Roux
75724 Paris Cedex 15
France

Summary

Spontaneous activity patterns in the developing retina appear important for the functional organization of the visual system. We show here that an absence of early retinal waves in mice lacking the $\beta 2$ subunit of the nicotinic acetylcholine receptor (nAChR) is associated with both gain and loss of functional organization in the dorsal lateral geniculate nucleus (dLGN). Anatomical studies show normal gross retinotopy in the $\beta 2^{-/-}$ dLGN but suggest reduced topographic precision in the retinogeniculate projection. Physiological recordings reveal normal topography in the dorsoventral visual axis but a lack of fine-scale mapping in the nasotemporal visual plane. In contrast, unlike wild-type mice, on- and off-center cells in the $\beta 2^{-/-}$ dLGN are spatially segregated. The presence of the $\beta 2$ subunit of the nAChR in the CNS is therefore important for normal functional organization in the retinogeniculate projection.

Introduction

The discovery of patterned spontaneous activity in the immature mammalian retina (Galli and Maffei, 1988; Meister et al., 1991) raised the hypothesis that this activity orders the development of retinal projections. Hebbian models show that patterns of retinal activity contain sufficient spatiotemporal information to drive refinement of retinotopy (Eglen, 1999; Butts, 2002), the segregation of inputs from the two eyes (Eglen, 1999; Butts, 2002), and the segregation of on- and off-center neurons (Lee et al., 2002) in structures that receive retinal projections. Is this activity necessary for normal visual development?

Direct investigations of retinal activity's developmental significance in the ferret have employed pharmacological manipulations to eliminate early spontaneous

activity. Between postnatal day 1 (P1) and P10 in this species, spontaneous activity is mediated by nicotinic cholinergic transmission (Feller et al., 1996; Penn et al., 1998) and, in the form of either action potential firing (Meister et al., 1991) or transient influxes of calcium (e.g., Feller et al., 1996), takes the form of waves that sweep periodically across the retina. Although calcium transients and action potentials are well correlated in normal retinae (Feller et al., 1996), they can be differentially affected by certain experimental manipulations (Huberman et al., 2003). For this reason, we will henceforth use the term "retinal waves" to refer only to activity assessed using calcium imaging. Epibatidine blockade of retinal nicotinic receptors from P1 to P10 eliminates both spike firing in retinal ganglion cells and retinal waves and prevents initial ocular segregation in the ferret dLGN (Penn et al., 1998). After a recovery period encompassing later glutamatergic spontaneous activity (Wong et al., 2000), the inputs from the two eyes do segregate, but not into characteristic eye-specific laminae (Huberman et al., 2002). Similarly, inputs from on- and off-center retinal ganglion cells also segregate in the epibatidine-recovery ferret dLGN but fail to form laminae (Huberman et al., 2002). Early cholinergic retinal waves are therefore critical for the normal lamination of the ferret dLGN. However, early epibatidine treatment has no effect on the ferret dLGN's retinotopicity (Huberman et al., 2002). This probably reflects the fact that retinal target structures are retinotopically organized at birth in this species (Chalupa and Snider, 1998; King et al., 1998).

A separate means of assessing the developmental significance of spontaneous retinal activity is offered by transgenic technology. Transmission through the dominant nicotinic acetylcholine receptor isoform in the brain is critically dependent on the presence of the $\beta 2$ subunit (Picciotto et al., 1995, 1998; Zoli et al., 1998). Mice that lack expression of this subunit ($\beta 2^{-/-}$) have no retinal waves from P1 to P7 (Bansal et al., 2000). During this period, retinal ganglion cells remain active, but correlations in spiking activity between neighboring neurons are drastically reduced (C.L. Torborg and M.B. Feller, 2003, Soc. Neurosci., abstract). Like epibatidine-treated ferrets, $\beta 2^{-/-}$ mice show disrupted lamination of inputs from the two eyes in the dLGN (Rossi et al., 2001) coupled with a fine-scale anatomical segregation of binocular inputs (Muir-Robinson et al., 2002). Again, early cholinergic waves appear essential for normal dLGN lamination. But are they necessary for other aspects of functional organization in the mouse visual system? Unlike the ferret, retinotopy in rodent retinal target structures is not present before waves begin (Simon and O'Leary, 1992a) and its development requires neuronal activity (Simon et al., 1992). This raises the distinct possibility that dLGN retinotopicity could be disrupted if cholinergic waves are blocked in mice. Whether the rodent dLGN displays any form of on/off organization and whether this organization is dependent upon spontaneous retinal waves are also both open questions, with recent studies showing that on/off responses can be hugely influenced

*Correspondence: ian.thompson@physiol.ox.ac.uk

³These authors contributed equally to this work.

⁴Present addresses: CNRS UMR 8544, Ecole Normale Supérieure, 46 rue d'Ulm, 75005 Paris, France, and CNRS UPR 1929, Institut de Biologie Physico-Chimique, 13 rue Pierre et Marie Curie, 75005 Paris, France.

by neuronal activity during development (Akerman et al., 2002; Tian and Copenhagen, 2003).

Here we explore the effects of the elimination of the $\beta 2$ subunit of the nAChR on the functional organization of the mouse dLGN, focusing on retinotopicity and the segregation of on- and off-responses. Anatomical and physiological approaches reveal normal gross retinotopy in the $\beta 2^{-/-}$ dLGN but disrupted fine mapping. Functionally, the $\beta 2^{-/-}$ dLGN displays a loss of fine retinotopicity in the nasotemporal visual axis. In contrast, $\beta 2^{-/-}$ mice show a gain of on/off organization: while on- and off-center cells are scattered randomly throughout the normal dLGN, in $\beta 2^{-/-}$ animals they cluster into cell type-specific domains.

Results

Anatomical Retinotopy

We analyzed the topographic distribution of retinogeniculate projections in wild-type (wt) and $\beta 2^{-/-}$ mice by examining dLGN terminal zones (TZs) labeled by focal injections of Dil tracer into the retina. At postnatal day 14, the age at which our observations were made, the wt topographical map is completely developed (Feldheim et al., 1998).

We found that $\beta 2^{-/-}$ retinogeniculate TZs are located in the correct region of the dLGN, but are weaker and more diffuse than those in wt animals. In wt mice, Dil injected into the temporal margin of the retina labels a highly focused and very dense zone of axonal arborization, the TZ, at the caudomedial edge of the dLGN, while Dil injected in the nasal retina labels a similarly focused TZ at the dLGN's rostromedial edge (Figure 1A). In $\beta 2^{-/-}$ mice, temporal retina also projects to the caudomedial edge of the dLGN and nasal retina to the rostromedial edge of the nucleus, indicating that the gross retinotopic map in the dLGN is not perturbed in these animals (Figure 1A). However, TZs in $\beta 2^{-/-}$ mice do appear larger, in all directions, compared to those in wt animals and also seem less densely labeled than their wt counterparts (Figure 1A). Furthermore, in a few cases (4/24 injections), the shape of the $\beta 2^{-/-}$ TZ was strikingly different from wt (Figure 1B). In these cases we observed a dispersed and patchy "island-like" distribution of terminal arbors that was never observed in wt animals (0/25 injections).

Quantification of TZ images confirmed the above observations. Measuring TZ areas showed that focal injections occupying around 1% of the wt retina labeled around 1% of the wt dLGN (nasal mean \pm SEM, 1.2% \pm 0.1% of the total dLGN area; temporal, 0.9% \pm 0.2%). In comparison, temporal and nasal axons from $\beta 2^{-/-}$ retinae covered dLGN areas approximately 2- to 4-fold larger than those in wt mice (nasal, 4.7% \pm 0.6%; temporal, 2.4% \pm 0.2%; Figure 1C). These differences were significant for both injection sites (t test, nasal $p = 0.0004$, temporal $p = 0.002$) and did not reflect a smaller overall dLGN area in $\beta 2^{-/-}$ animals (wt, 0.48 \pm 0.01 mm²; $\beta 2^{-/-}$, 0.49 \pm 0.01 mm²; t test, $p = 0.38$) nor larger injection sites in the mutant mice (see Experimental Procedures).

Image analysis of labeling density also revealed differ-

ences between the two groups (Figure 1D). TZ densities were significantly lower in $\beta 2^{-/-}$ mice for both temporal (wt OD, 0.26 \pm 0.04; $\beta 2^{-/-}$, 0.15 \pm 0.02; t test, $p = 0.017$) and nasal (wt OD, 0.33 \pm 0.03; $\beta 2^{-/-}$, 0.23 \pm 0.03; t test, $p = 0.036$) injections. This result suggests that the increase in size observed in $\beta 2^{-/-}$ TZs is not caused by an increase in the number of axon branches, but rather by less precise local mapping in the retinogeniculate projection.

We attempted to assess whether this lack of local anatomical precision was more pronounced in either the nasotemporal or dorsoventral visual axis. In horizontal sections, the width of retinogeniculate TZs was measured in the posteromedial-anterolateral and posterolateral-anteromedial axes of the dLGN, which approximate to the representations of the nasotemporal and dorsoventral retinal dimensions, respectively (Figure 3; Feldheim et al., 1998). TZ widths were expressed as percentages of total dLGN length in the appropriate axis. While $\beta 2^{-/-}$ TZs were expanded in both visual axes relative to their wt counterparts, and while this expansion relative to wt TZs was more pronounced in the nasotemporal axis, these differences were not significant (nasotemporal axis: wt mean \pm SEM, 11.2% \pm 2.3%; $\beta 2^{-/-}$, 16.8% \pm 4.2%; t test, $p = 0.26$; dorsoventral axis: wt, 23.9% \pm 3%; $\beta 2^{-/-}$, 25.3% \pm 2.8%; t test, $p = 0.73$). Our anatomical data therefore show that local retinotopy is disrupted in the $\beta 2^{-/-}$ dLGN at P14 but cannot determine whether this disruption is more pronounced in a particular visual axis. For this, we turned to an analysis of functional retinotopic mapping in the dLGN of adult $\beta 2^{-/-}$ mice.

Functional Retinotopy

To address how anatomical disruption alters functional retinotopy in the $\beta 2^{-/-}$ dLGN, we recorded single dLGN cell visual responses in vivo in anesthetized adult wt and $\beta 2^{-/-}$ mice. Comparing functional retinotopy across wt and $\beta 2^{-/-}$ animals was possible because, in terms of general RF structure, we saw no difference between wt and $\beta 2^{-/-}$ dLGN cells (Figure 2). As in wt animals (Figure 2A; Grubb and Thompson, 2003), all $\beta 2^{-/-}$ RFs that could be quantitatively mapped with reverse correlation were dominated by a clearly localized, roughly circular center mechanism that responded to either increases (on) or decreases (off) in stimulus luminance (Figure 2B). Furthermore, neither the proportion of RFs that could be quantitatively mapped (wt, 87/132 = 66%; $\beta 2^{-/-}$, 121/184 = 66%; Fisher's exact test, $p = 1$) nor the relative numbers of on- and off-center RFs (wt, 48 on-center, 39 off-center; $\beta 2^{-/-}$, 80 on-center, 41 off-center; Fisher's exact test, $p = 0.11$) differed significantly between the two groups.

Qualitative observations from our recordings confirmed our first anatomical result: the retinotopic map is grossly normal in the $\beta 2^{-/-}$ dLGN. In wt mice, receptive fields (RFs) in the nasal visual field (corresponding to temporal retina) were obtained from neurons located in the caudomedial dLGN, while dorsal RFs (corresponding to ventral retina) were recorded from cells found in rostromedial portions of the nucleus (Figure 3A; Metin et al., 1983; Wagner et al., 2000). An identical rough map

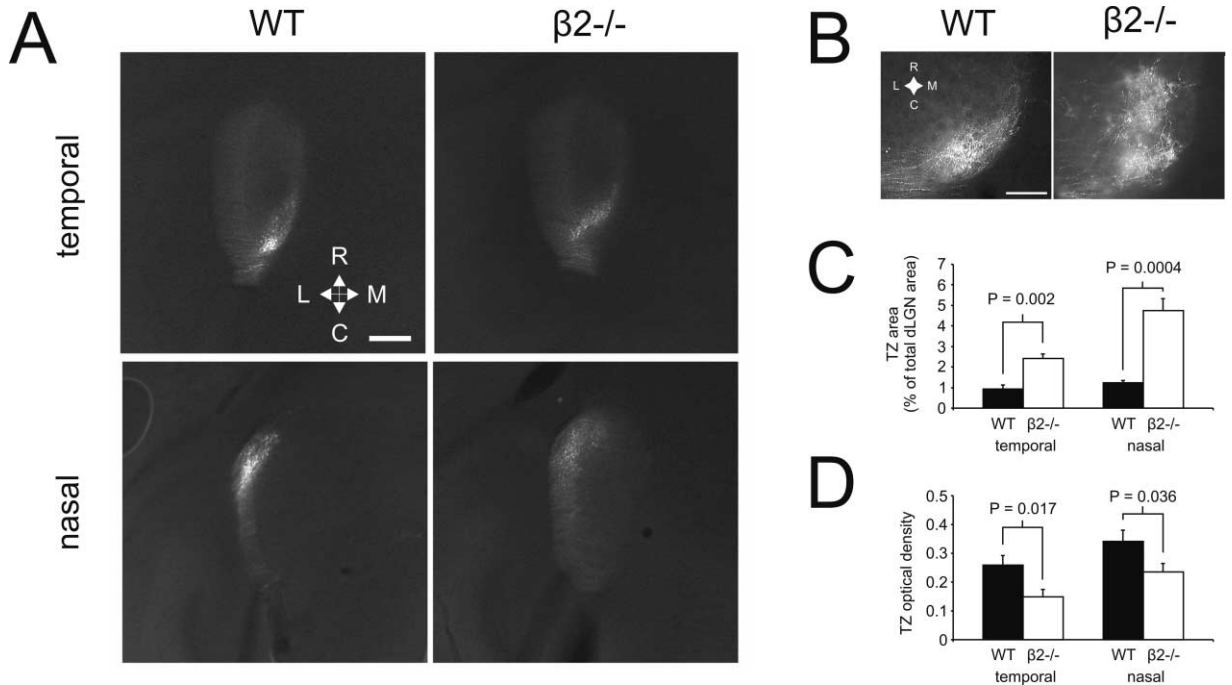


Figure 1. Projections from Small Areas of the Retina Target the Correct Region of the dLGN but Are Weaker and More Diffuse in $\beta 2^{-/-}$ Mice (A) Retinogeniculate terminal zones (TZs) labeled by focal Dil injections into nasal or temporal retina show that $\beta 2^{-/-}$ mice have grossly normal retinotopicity in this projection. Nasal retina projects to caudomedial dLGN, while temporal retina projects to rostralateral dLGN. TZs in $\beta 2^{-/-}$ mice, however, appear less dense and slightly enlarged compared to those in wt mice. Abbreviations: R, rostral; C, caudal; L, lateral; M, medial. Scale bar equals 250 μ m. (B) TZs imaged under higher magnification. At this scale, patchy, island-like TZs were sometimes observed in $\beta 2^{-/-}$ mice but were never seen in wt animals. Orientation as in (A). Scale bar equals 100 μ m. (C) Quantification of TZ size. Following focal injections in both nasal and temporal retina, retinogeniculate TZs were significantly larger in $\beta 2^{-/-}$ than in wt mice. Bars show means; error bars show SEMs. (D) Quantification of TZ density. TZs from both nasal and temporal retina are less dense in $\beta 2^{-/-}$ than in wt mice. Bars show means; error bars show SEMs.

was present in $\beta 2^{-/-}$ mice and could be reliably used to direct electrode placements. If we were recording from cells with nasal RFs, for example, we knew we were near the medial edge of the dLGN and that any subsequent penetrations should be aimed more laterally.

However, since our Dil tracing data suggest subtle anomalies in the $\beta 2^{-/-}$ retinogeniculate projection at a local level, we wanted to quantitatively assess fine functional retinotopy in the wt and $\beta 2^{-/-}$ dLGN. Our analysis involved pairs of cells recorded on the same penetration whose RFs could be mapped objectively (Figure 2; see Experimental Procedures) with the stimulus display in exactly the same location. For each such cell pair, we knew the separation distance of the constituent units in the dLGN and the relative positions of their RFs in both the nasotemporal and dorsoventral visual dimensions (Figure 3B, see Experimental Procedures). If our electrode penetrations were angled appropriately, correlating cell separation with RF separation across all pairs should provide a quantitative measure of local mapping: in a retinotopically organized structure, larger cell separations should be associated with bigger RF displacements.

In both the nasotemporal and dorsoventral visual di-

mensions, our wt data showed just those characteristics (Figure 3C). On average, as the electrode moved ventrally through the dLGN, RFs moved ventrally and nasally in visual space, and at larger cell separations, these RF position changes were larger too. The maps were by no means perfect—especially at small separations we often saw RF movements in the “wrong” direction—but linear regression of the two wt plots revealed highly significant relationships between cell and RF separation in both dimensions (dorsoventral, $r = -0.58$, $p < 0.0001$; nasotemporal, $r = -0.3$, $p = 0.0007$; $n = 123$).

In $\beta 2^{-/-}$ mice, however, one of the maps is missing (Figure 3C). The fine-scale map of dorsoventral visual space appears entirely normal: as the electrode moved more ventrally in the dLGN, so RFs moved ventrally in the visual field ($r = -0.41$, $p < 0.0001$, $n = 110$). Furthermore, these $\beta 2^{-/-}$ data were statistically indistinguishable (see Experimental Procedures) from those in the wt dorsoventral plot. In the nasotemporal dimension, though, there is no fine-scale map whatsoever. We saw no relationship between dLGN cell separation and RF separation in nasotemporal visual space in $\beta 2^{-/-}$ mice ($r = -0.01$, $p = 0.88$). This effect is not due to general differences between our wt and $\beta 2^{-/-}$ data: the groups were no different in terms of physiology, optics, eye

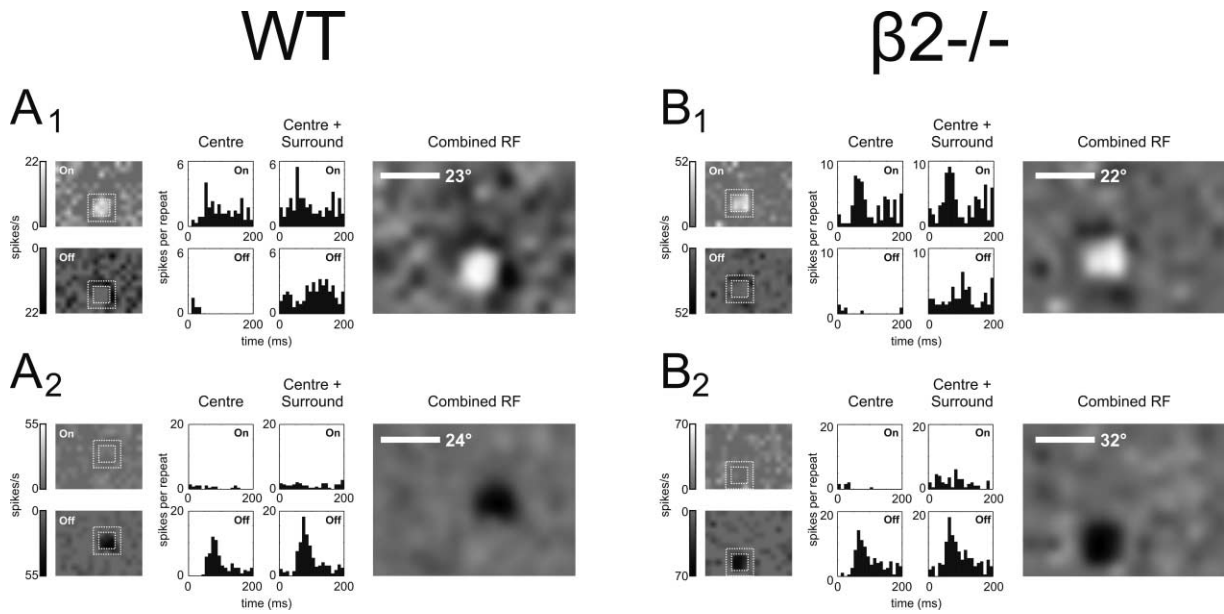


Figure 2. Neurons in the $\beta 2^{-/-}$ dLGN Have Normal Receptive Field Structure

(A) Examples of dLGN receptive fields (RF) in wt mice. RFs that could be mapped quantitatively using reverse correlation were dominated by a roughly circular on (A_1) or off (A_2) center mechanism (Grubb and Thompson, 2003), with evidence of an antagonistic surround mechanism in some cases (A_1). For each cell, a series of plots is presented. In raw response-weighted profiles (left), the intensity of each pixel reflects the strength of the cell's response, as indicated in the grayscale key, to a flashed white (on) or black (off) square centered on that location. Poststimulus time histograms (middle) show the number of spikes per stimulus run recorded in responses to white (on) and black (off) flashed squares. "Center" histograms show responses to stimuli centered in the inner dashed square superimposed on the raw response-weighted profiles, while "Center + Surround" histograms show responses to stimuli centered within the outer dashed square. To produce the combined RF profile (right), each raw off profile was subtracted from the corresponding raw on profile and the resulting map was smoothed with a Gaussian filter (see Experimental Procedures). Scale bars represent varying degrees of visual angle (23° in A_1 , 24° in A_2) because the viewing distance of the stimulus display varied from cell to cell.

(B) Examples of dLGN RFs in $\beta 2^{-/-}$ mice. As in wt animals, RFs obtained with reverse correlation were on- (B_1) or off- (B_2) center, sometimes with evidence of an antagonistic surround (B_1). All conventions as in (A).

movements, or penetration angle (see Experimental Procedures). In $\beta 2^{-/-}$ mice, therefore, anatomical disruption of local dLGN retinotopy (Figure 1) is coupled with a dimension-specific loss of local functional retinotopic organization.

On/Off Organization

It is known that alterations in neuronal activity early in development can affect the representation of individual cells' on and off responses in the mouse retina (Tian and Copenhagen, 2003) and ferret dLGN (Akerman et al., 2002). We know from our present functional data that the $\beta 2^{-/-}$ mutation has no effect on the on/off properties of individual dLGN cells: all recorded cells in both wt and $\beta 2^{-/-}$ mice were either on- or off-dominated. However, in mustelids, on- and off-center cells are located in different functional subdivisions of the dLGN (Stryker and Zahs, 1983). We postulated that the wt mouse dLGN might also show such on/off organization and that this organization might be disrupted in $\beta 2^{-/-}$ animals. In fact, our functional data revealed precisely the opposite effect. While on- and off-center cells are arranged randomly within the wt mouse dLGN, the $\beta 2^{-/-}$ dLGN contains significant on/off organization.

Penetrations through the wt dLGN usually produced a mixture of on- and off-center cells, with successive units seemingly arranged at random. In stark contrast,

penetrations in $\beta 2^{-/-}$ mice produced sequences of cells of the same center type, as if we were passing through clusters of on-center or off-center neurons (Figure 4A). To quantify these observations, we first compared the length of these same center-type sequences in wt and $\beta 2^{-/-}$ mice (Figure 4B). While almost all runs of same center-type cells in wt penetrations were less than 150 μm long, we often recorded from exclusively on- or off-center cells for more than 150 μm in the $\beta 2^{-/-}$ dLGN. Mean same center-type run length was significantly greater in $\beta 2^{-/-}$ mice than in wt animals (wt mean \pm SEM, $101 \pm 11 \mu\text{m}$; $\beta 2^{-/-}$, $155 \pm 18 \mu\text{m}$; t test with Welch correction, $p = 0.013$).

To look more closely for evidence of on/off organization, we also analyzed the neighbor relations of each on- or off-center cell we recorded on a particular penetration. If on- and off-center cells are arranged randomly in the dLGN, the probability that the nearest neighbor of a given cell is of the same center type is determined, in a simple binomial model, by the relative numbers of on- and off-center cells in a given sample (see Experimental Procedures). In our sample of 85 wt cells (47 on and 38 off), 43 should have a nearest neighbor of the same center type if center type organization is completely random in the dLGN. Indeed, 47/85 wt cells had a same-type nearest neighbor (Figure 4C), a proportion not significantly different from that predicted by the bi-

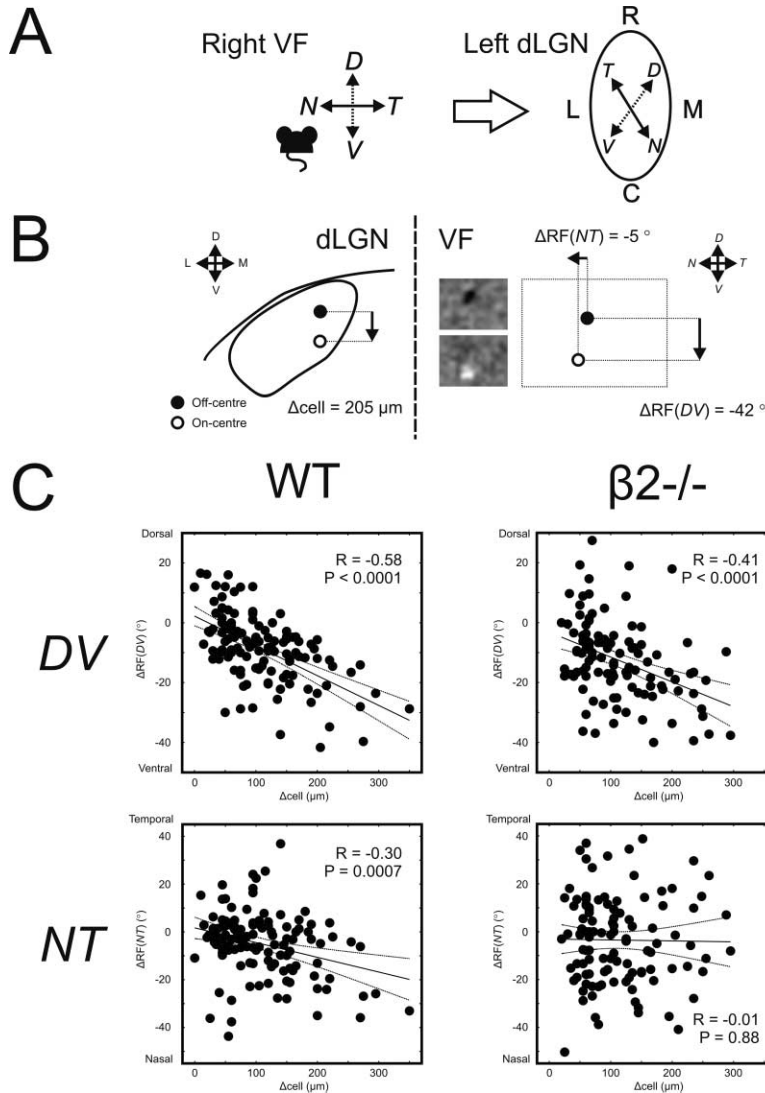


Figure 3. Fine-Scale Retinotopic Mapping Is Disrupted in the $\beta 2^{-/-}$ dLGN in the Naso-temporal Direction Only

(A) The rough retinotopic map is normal in the $\beta 2^{-/-}$ dLGN. In both wt and $\beta 2^{-/-}$ mice, dorsal→ventral visual space is mapped in rostromedial→caudolateral dLGN, while nasal→temporal visual space is mapped in caudomedial→rostromedial dLGN (Metin et al., 1983; Wagner et al., 2000). VF, visual field; D, dorsal; V, ventral; N, nasal; T, temporal; other conventions as in Figure 1.

(B) Assessing fine-scale retinotopic mapping using pairs of cells. On a given penetration we often mapped receptive fields (RFs, see Experimental Procedures) of different cells with the stimulus screen in exactly the same location, allowing us to correlate the separation of cell pairs in the dLGN ($=\Delta \text{cell}$) with the separation of their RFs in nasotemporal ($=\Delta \text{RF}(NT)$) and dorsoventral ($=\Delta \text{RF}(DV)$) visual space. All conventions as in (A).

(C) Functional retinotopic maps in wt and $\beta 2^{-/-}$ mice. Along the average dorsal→ventral penetration in wt mice, RF position varied systematically in both dimensions, moving more ventral and more nasal in visual space. In $\beta 2^{-/-}$ mice, the DV map was present: greater separations of cell pairs in the dLGN were associated with greater dorsal→ventral RF movements in the visual world. However, the NT map was completely absent: we saw no significant relationship between dLGN cell separation and RF movement in this dimension. In each plot each dot represents one cell pair (wt $n = 123$; $\beta 2^{-/-}$ $n = 110$), solid lines show the best fitting linear regression of the data, and dotted lines show the 95% confidence interval of this fit.

nomial model (Fisher's exact test, $p = 0.65$). On- and off-center cells in the wt dLGN are indeed scattered randomly in the nucleus. In $\beta 2^{-/-}$ mice, the sample of 81 on-center cells and 38 off-center cells led us to expect 67/119 same-type nearest neighbor cells if cell-type organization were random. We actually saw 89/119 such cells, a significantly greater proportion than predicted (Fisher's exact test, $p = 0.004$; Figure 4C). Thus, unlike the wt dLGN, on- and off-center cells in $\beta 2^{-/-}$ mice are significantly clustered together.

The above nearest neighbor analysis, however, addresses only the relationships between cells closest to one another. We extended our description of on/off organization in the $\beta 2^{-/-}$ dLGN to all pairs of cells recorded on the same penetration using the following reasoning: if there is on/off clustering, the average distance between cells of the same center type should be less than that between cells of the opposite center type. Indeed, in $\beta 2^{-/-}$ animals, the mean separation between cells that shared a common RF center type was, at $127 (\pm 7) \mu\text{m}$, significantly smaller than that between cells that had different RF center types ($172 (\pm 15) \mu\text{m}$; t test, $p =$

0.0093). In wt mice, there was no difference in separation between these two groups (same, $143 (\pm 9) \mu\text{m}$; different, $152 (\pm 11) \mu\text{m}$; t test, $p = 0.52$; Figure 4D). All the above analyses combine to provide convincing evidence that while the wt dLGN contains randomly distributed on- and off-center cells, the dLGN in $\beta 2^{-/-}$ mice has gained supernormal on/off organization.

Ocularity

We assessed the ocularity of single cell responses in the wt and $\beta 2^{-/-}$ dLGN using vertical drifting sinusoidal gratings presented to the receptive field. Under binocular viewing conditions, these stimuli elicited responses that were phase-locked to one half of each grating cycle. By covering just one eye, we could always make these phase-locked responses disappear in all wt and $\beta 2^{-/-}$ neurons tested. With the opposite eye covered, the same pattern of responses seen under binocular conditions returned (Figure 5). In our sample, then, every wt and $\beta 2^{-/-}$ dLGN cell was monocularly driven. In wt mice, these tests revealed 39 cells driven solely through the contralateral eye and 12 driven solely through the ipsilat-

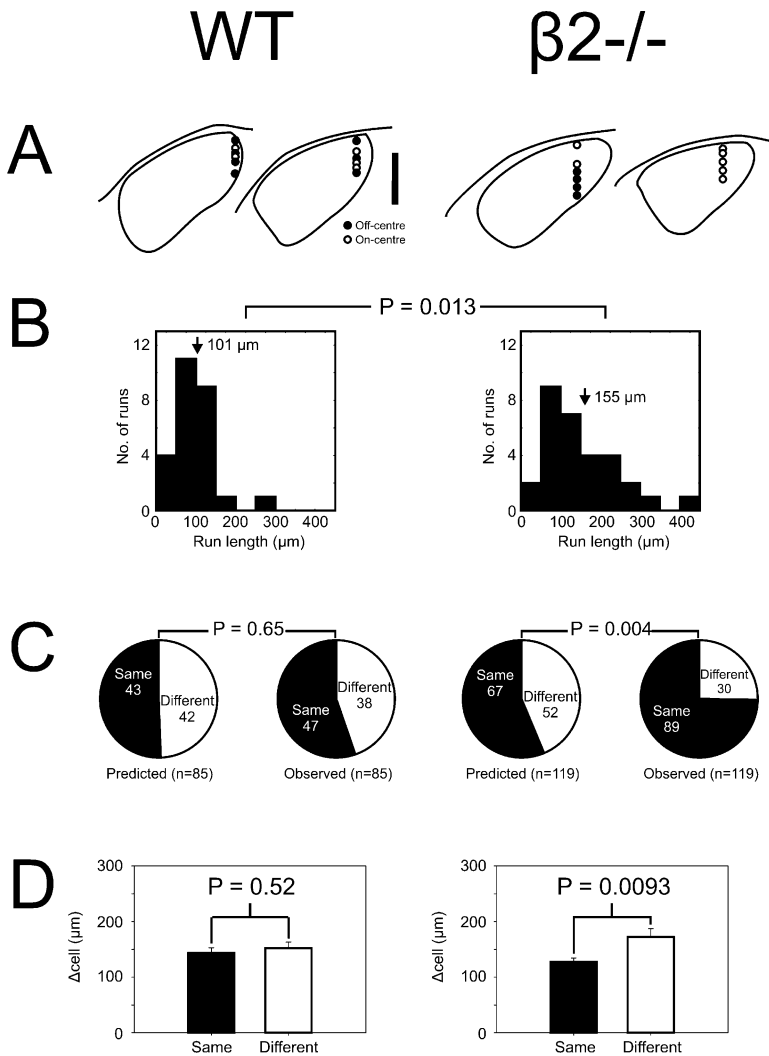


Figure 4. On- and Off-Center dLGN Cells Are Segregated in $\beta 2^{-/-}$, but not in Wild-Type Mice

(A) Patterns of on- and off-center cells encountered on single penetrations through the dLGN of wt and $\beta 2^{-/-}$ animals. Each outline of the dLGN and its overlying optic tract is shown in coronal section. While on- and off-center cells appear intermingled within the wt dLGN, they appear segregated in the $\beta 2^{-/-}$ dLGN. Scale bar equals 400 μm .

(B) Runs of consecutive cells of the same center type are longer in the $\beta 2^{-/-}$ dLGN. Histograms show almost all wt run lengths clustered around 100 μm , while $\beta 2^{-/-}$ penetrations produced many run lengths greater than 150 μm . The means of the two distributions, marked by arrows, are significantly different.

(C) Nearest-neighbor analysis of on/off organization in the dLGN. In wt mice, the proportion of dLGN cells whose nearest recorded neighbor shared the same center type was no different than would be predicted if on- and off-center cells were mixed randomly throughout the nucleus. In $\beta 2^{-/-}$ mice, on the other hand, we saw significantly more same-neighbor cases than would be predicted by such a model.

(D) Comparison of the mean separations of cell pairs in which constituent neurons had the same or different RF center types. Error bars show SEM. No difference was seen between the two groups in wt animals (mean (\pm SEM): same, 143 (\pm 9) μm ; different, 152 (\pm 11) μm), but in $\beta 2^{-/-}$ mice, cells with similar RF center types were located significantly closer to each other than cells with different RF center types (same, 127 (\pm 7) μm ; different, 172 (\pm 15) μm).

eral eye. In $\beta 2^{-/-}$ mice, we found 29 contralaterally and 6 ipsilaterally driven cells. These proportions were not significantly different across the two groups (Fisher's exact test, $p = 0.59$). We already knew from anatomical tracing studies that although ocular lamination of the dLGN is disrupted in $\beta 2^{-/-}$ mice (Rossi et al., 2001), segregation of afferents from the two eyes still occurs (Muir-Robinson et al., 2002). We now know that this segregation takes place to the finest possible resolution: the level of the single cell.

We did not record from enough ipsilaterally driven cells to be able to estimate the size of ipsilateral domains in $\beta 2^{-/-}$ mice. We did, however, notice that while single unit activity at a particular location in the $\beta 2^{-/-}$ dLGN responded only to input from one eye, some of the background multiunit activity (which we could still hear while recording spikes from a single neuron) responded to input from the *other* eye. Such binocular multiunit activity was never observed in the wt dLGN, suggesting that eye-specific domains are smaller in $\beta 2^{-/-}$ mice.

Independence of Functional Attributes

The $\beta 2^{-/-}$ dLGN displays a lack of fine-scale topography in the nasotemporal retinal axis (Figure 3), novel on/off

organization (Figure 4), and disrupted ocular lamination (Rossi et al., 2001; Muir-Robinson et al., 2002). Are any of these features interdependent? For instance, if the nasotemporal retinal axis were mapped in an orderly fashion *within* a functional domain (ocular, or on/off) but the maps between domains were out of register, this could explain the observed breakdown in local functional topography (Figure 3). We now show that this is not the case: functional attributes in the $\beta 2^{-/-}$ dLGN appear to be organized independently of one another.

Our analysis of functional retinotopy (Figure 3) included data from both ipsi- and contralaterally driven cells. Could each of these cell types have had their own, independent map of nasotemporal visual space in the $\beta 2^{-/-}$ dLGN, with overall topography disrupted only because of abnormal ocular lamination (Rossi et al., 2001; Muir-Robinson et al., 2002)? It appears not. Although we recorded from too few ipsilaterally driven cells to address retinotopy within their domains, nasotemporal mapping solely within contralaterally driven cells was absent in the $\beta 2^{-/-}$ dLGN ($r = 0.24$, $p = 0.21$, $n = 29$). In addition, relationships between cell separation and RF displacements in same-eye versus different-eye cell pairs were statistically indistinguishable (see Experi-

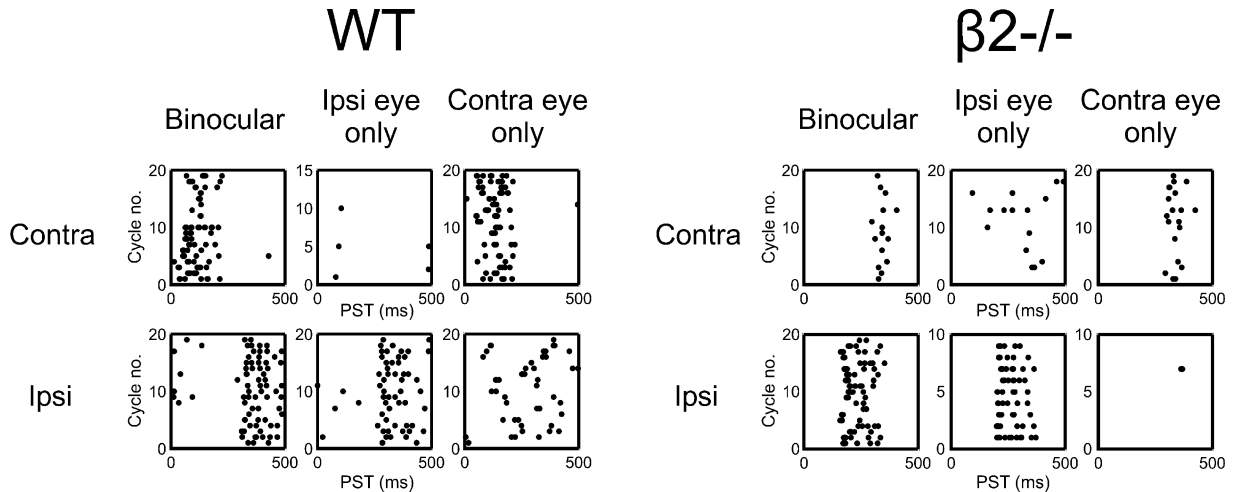


Figure 5. Examples of Monocularly Driven dLGN Cells in Wild-Type and $\beta 2^{-/-}$ Mice

Raster plots show dLGN cell responses to vertical drifting sinusoidal gratings (spatial frequency $0.03c^\circ$, temporal frequency 2 Hz, contrast 70%) under binocular viewing conditions (left), with the contralateral eye covered (center), and with the ipsilateral eye covered (right). Binocular responses are phase-locked to one half of the stimulus cycle. In contralateral cells (top), these responses disappear entirely or are replaced with random spontaneous firing when the contralateral eye is covered, but reappear completely when the cover is switched to the ipsilateral eye. In ipsilaterally driven cells (bottom) the opposite pattern of results is observed. Each dot represents one action potential. PST, poststimulus time; Contra, contralateral; Ipsi, ipsilateral.

mental Procedures) in both visual dimensions in wt and in $\beta 2^{-/-}$ animals. Ocularity and retinotopy appear to be independently organized in the wt and $\beta 2^{-/-}$ dLGN.

A similar analysis in respect of the on/off domains shows that the gain of organization in the $\beta 2^{-/-}$ dLGN (Figure 4) is not related to the loss of fine-scale retinotopic mapping in these mice (Figure 3). Neither exclusively on- nor exclusively off-center pairs show nasotemporal topography (on-center pairs, $r = -0.02$, $p = 0.86$, $n = 64$; off-center pairs, $r = 0.053$, $p = 0.82$, $n = 21$), but both domains display a dorsoventral map (on-center pairs, $r = -0.41$, $p = 0.0008$, $n = 64$; off-center pairs, $r = -0.62$, $p = 0.003$, $n = 21$). Furthermore, we saw no significant differences in wt or $\beta 2^{-/-}$ mice, in either retinotopic dimension, between maps generated from same center-type cell pairs and those generated from different center-type cell pairs (see Experimental Procedures). This implies that fine-scale retinotopic maps are just as good (or as bad) across RF center-type boundaries as they are within them. As far as we can tell with our current data set, therefore, on/off organization and fine-scale retinotopic mapping in the dLGN of wt and $\beta 2^{-/-}$ mice are independent processes.

Finally, we saw no interdependence of on/off organization and ocular organization in wt or $\beta 2^{-/-}$ mice. In wt animals, on- and off-center cells could be found within individual ipsilateral or contralateral domains. In $\beta 2^{-/-}$ mice, ipsi- and contralaterally driven cells could be found within individual on- or off-center domains. There was also no evidence that on/off organization in $\beta 2^{-/-}$ mice somehow replaced the missing ocular organization in these animals. Our observations were inconsistent with there being an on- or off-center "island" in the medial dLGN in these animals: both on- and off-center types were encountered at all dLGN locations, and despite the overall large-scale segregation, we sometimes saw three changes of RF center type along a single

penetration. on/off organization in $\beta 2^{-/-}$ mice occurs when the dLGN is abnormally organized according to ocularity, but it does not simply "plug in" to a vacant ocular framework.

Discussion

We have shown that $\beta 2^{-/-}$ mice have a loss of fine topography, but a gain of on/off organization in the dLGN.

A Retinal Locus of Effect?

The $\beta 2$ subunit of the nicotinic acetylcholine receptor (nAChR) is present at high levels throughout the mouse brain, particularly in the thalamus (Zoli et al., 1998), suggesting that the phenotype we observed could be due to the absence of the $\beta 2$ subunit in this brain area. However, we would argue that the above effects are most parsimoniously explained with reference to abnormalities in the $\beta 2^{-/-}$ retina, for a number of reasons. First, in the adult dLGN, acetylcholine (ACh) plays an important role in modulating neuronal responses, increasing levels of spontaneous and visually driven activity (e.g., Sillito et al., 1983; Eysel et al., 1986; Francesconi et al., 1988). These effects could arise from nAChRs that act postsynaptically to depolarize both local interneurons (e.g., Zhu and Uhlrich, 1997) and thalamocortical relay cells (e.g., McCormick and Prince, 1987; McCormick and Pape, 1988; Zhu and Uhlrich, 1997). ACh, via nAChRs, also acts presynaptically to increase transmitter release at intrathalamic (Lena and Changeux, 1997) and probably retinogeniculate (Swanson et al., 1987; Prusky and Cynader, 1988; King, 1990) synapses. However, these actions of ACh in the *adult* should not directly alter the functional organization of the dLGN. While $\beta 2$ subunit containing nAChRs may modulate activity levels in the nucleus, such cholinergic modulation should

never alter a cell's receptive field location or center type, both of which are determined by "driving" retinal inputs (Sherman and Guillery, 2002).

On the other hand, changes in cholinergic activity caused by the $\beta 2^{-/-}$ manipulation could have rather different effects in the *developing* dLGN. nAChRs are present throughout the pre- and postnatal development of the rodent brain (e.g., Naeff et al., 1992), such that the effects of the $\beta 2^{-/-}$ mutation could occur at many stages of neural development. Indeed, in the frog tectum, cholinergic transmission is necessary for map development and maintenance (Edwards and Cline, 1999; Yu et al., 2003). However, blocking nAChRs in the developing rat superior colliculus does not affect the establishment of topography (Simon et al., 1992), and blocking nAChRs in the developing ferret dLGN does not prevent the formation of ocular laminae (Penn et al., 1998). Thus, at least postnatally, nAChR activity in the target is not necessary for some of the developmental processes in the mammalian retinal pathway. In addition, while we did see loss of a nasotemporal retinotopic map in the $\beta 2^{-/-}$ dLGN, this was not due to a general loss of plasticity in the retinogeniculate projection: we observed a *gain* in organization according to cell center type, and we knew already that initially disordered retinal projections in this mutant are able to organize themselves into segregated eye-specific microdomains (Muir-Robinson et al., 2002). Developmental plasticity is thus still possible in the postnatal $\beta 2^{-/-}$ dLGN. Furthermore, although developmental effects of the $\beta 2^{-/-}$ mutation prior to birth cannot be ruled out, we would argue that the subtle nature of the abnormalities reported here make this less likely.

Finally, the anatomical and functional $\beta 2^{-/-}$ phenotype is strikingly similar to that seen in the ferret dLGN after pharmacological blockade of nAChRs in the immature retina (Huberman et al., 2002). Both manipulations produce ocular segregation in the absence of lamination (Rossi et al., 2001; Huberman et al., 2002; Muir-Robinson et al., 2002), normal dorsoventral retinotopy (present data; Huberman et al., 2002), and nonlaminar on- or off-center domains that cross ocular boundaries (present data; Huberman et al., 2002). Indeed, these two different approaches in two different species produce different results in only one respect: a lack of fine nasotemporal retinotopy in the $\beta 2^{-/-}$ mouse. This single discrepancy could occur because developing rodent retinofugal projections show no initial nasotemporal ordering, unlike those of their carnivore predators (Simon and O'Leary, 1992a; Chalupa and Snider, 1998; King et al., 1998). Such phenotypic similarity between two different manipulations strongly suggests that their effects occur primarily in the only structure they both directly alter—the retina. However, although we would argue that abnormal functional organization in the $\beta 2^{-/-}$ dLGN is probably caused by abnormal spike activity in the early postnatal retina, we cannot definitely rule out potential contributions to the phenotype from pre- or postnatal nAChR-dependent processes in the dLGN itself.

Means of Possible Retinal Effects—Waves and Spikes

As assessed with calcium imaging, $\beta 2^{-/-}$ mice lack spontaneous retinal waves from P1 to P7 (Bansal et al.,

2000; Muir-Robinson et al., 2002). However, this does not necessarily mean that, in terms of spike activity, retinal ganglion cells are completely silent during this period in these animals. Although epibatidine, which acts on the type of nAChRs rendered nonfunctional by the $\beta 2^{-/-}$ mutation, eliminates both waves and retinal ganglion cell (RGC) spikes in the immature ferret retina (Penn et al., 1998), waves and RGC spikes need not go hand in hand. Immunotoxin depletion of amacrine cells in neonatal ferrets eliminates waves completely without altering overall levels of retinal ganglion cell firing (Huberman et al., 2003). This leaves open the possibility that while wave activity is lacking in the P1–P7 $\beta 2^{-/-}$ retina, RGC spikes continue as normal. In actual fact, recent evidence shows that RGCs do fire action potentials in the P1–P7 $\beta 2^{-/-}$ retina. Over this period in $\beta 2^{-/-}$ mice, correlations in firing between neighboring RGCs are drastically reduced, while overall firing rates are altered compared to wt animals (C.L. Torborg and M.B. Feller, 2003, Soc. Neurosci., abstract).

What does this mean in terms of the data we present here? Even if the effects of the $\beta 2^{-/-}$ mutation on functional organization in the dLGN really are retinal in origin, we share a problem with other studies in which manipulations affected both retinal waves and RGC firing rates (e.g., Penn et al., 1998; Rossi et al., 2001; Huberman et al., 2002; Muir-Robinson et al., 2002). We cannot be sure whether the abnormalities of functional organization we report are caused by a lack of patterning in retinal activity or simply a change in overall levels of retinal firing. This is particularly relevant where we observe missing functional organization in the $\beta 2^{-/-}$ dLGN—fine nasotemporal retinotopy could be lacking through either mechanism. But what is clear is that a given alteration in nAChR activity can have different effects on different aspects of dLGN development. Fine retinotopy in the nasotemporal axis is susceptible to alterations in nAChR activity that occur in $\beta 2^{-/-}$ mice, but fine retinotopy in the dorsoventral axis is not. The mechanisms that build fine retinotopy in different dimensions in the dLGN are thus distinct and separable. That a knockout mutation can produce a "supranormal" functional organization, on- and off-center domains, was also an unexpected result and shows that disruptions of normal synaptic processes can produce gains as well as losses in the functional organization of the visual system. This observation merits further investigation. It will be important, in particular, to determine when this organization appears. Is it directly induced by the RGC activity patterns seen in $\beta 2^{-/-}$ mice, in which case there should be evidence of segregation very early in development? Or are those activity patterns simply permissive for a subsequent sculpting of the projections, as we argue below? In conclusion, it is important to address the issue of instructive versus permissive roles for neuronal activity during development (Huberman et al., 2003), but even manipulations that cannot distinguish between these two roles can still be extremely informative. In the same vein, the phenotypic patterns produced by whole-animal genetic manipulations can still teach us much concerning neuronal development, even if we cannot be sure of the precise locus of their effects.

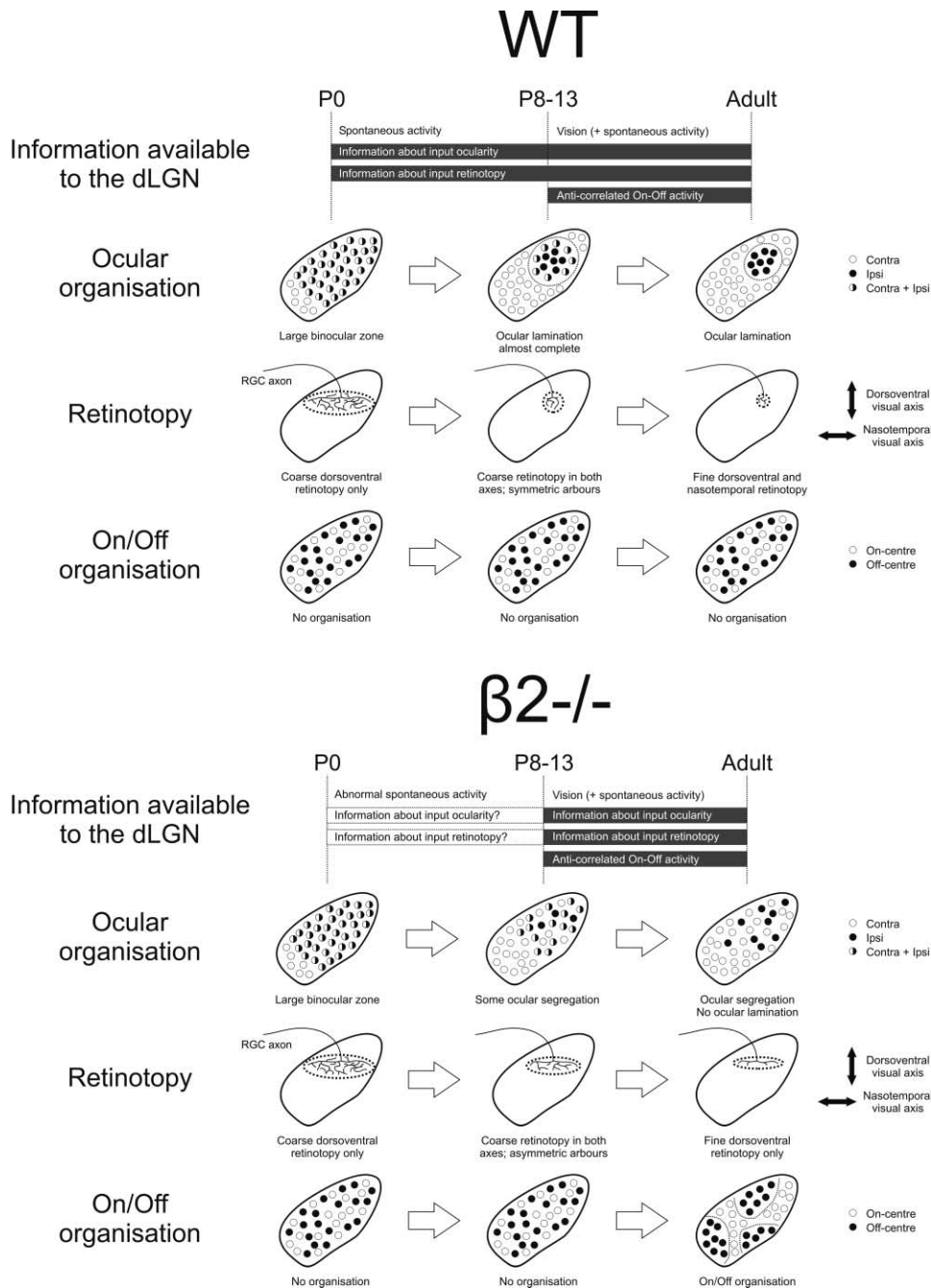


Figure 6. A Possible Model for the Development of Functional Organizational Features in the Wild-Type and $\beta 2^{-/-}$ dLGN

The model approximates three aspects of functional organization—ocular organization, retinotopy, and on/off organization—during the development of the dLGN in wt and $\beta 2^{-/-}$ mice. While we have striven for accuracy wherever possible in this figure, we should emphasize that it contains much conjecture and represents one way in which things *might* happen. We believe that on- and off-center-specific domains might form in the $\beta 2^{-/-}$ dLGN because of the relatively unstructured nature of the nucleus when it first receives anticorrelated on- and off-center activity. In wild-type (wt) mice, spontaneous activity in the two eyes in the first postnatal week may be responsible for the almost complete ocular lamination of the dLGN at P8 (Muir-Robinson et al., 2002). It is likely that retinotopy is rather well established in the mouse dLGN at this age, too (Simon and O'Leary, 1992a). Because the dLGN is already partly functionally organized by P8, when anticorrelated on-off activity reaches the dLGN in the second postnatal week via visually (Bonaventure and Karli, 1968; Akerman et al., 2002) or spontaneously (Wong and Oakley, 1996) evoked firing, the scope for organization of on- and off-center domains will be reduced. In contrast, the functional organization of the LGN at this stage in the $\beta 2^{-/-}$ mice is much more diffuse both in ocularity (Muir-Robinson et al., 2002) and retinotopy. With a relatively “blank slate” to work on—no major ocular or retinotopic organization to overcome—anticorrelated on-off activity may be in a much better position to shape the development of the $\beta 2^{-/-}$ dLGN. Large clusters of exclusively on- or exclusively off-center cells, along with nonlaminated ocular segregation and disrupted local retinotopic mapping in the nasotemporal visual axis, can form.

Explaining Specific Abnormalities of Functional Organization in the $\beta 2^{-/-}$ dLGN

The loss of fine topography in the $\beta 2^{-/-}$ dLGN is consistent with models showing that waves of spontaneous retinal activity can contribute to the refinement of retinotopicity in retinal target structures (Eglen, 1999; Butts, 2002). But why do $\beta 2^{-/-}$ mice lose functional topography in only one visual axis? The answer may lie in the anatomy of the rodent visual pathway: optic tract fibers entering the rat superior colliculus show some order in the dorsoventral, but not in the nasotemporal, retinal axis (Simon and O'Leary, 1991, 1992b). If we assume a similar bias upon entry to the dLGN in mice, fine topography in that initially highly disordered nasotemporal axis may be far more susceptible to alterations of spontaneous retinal activity. If this is the case, though, why do we not see asymmetric expansions in retinal terminal zones? These were larger in $\beta 2^{-/-}$ than in wt mice, but not significantly larger along the nasotemporal axis (Figure 1A). We can think of two possible explanations. The first is the age difference between our anatomical and physiological studies. Maybe pruning of axon arbors is not complete by P14 (Chen and Regehr, 2000), the age at which retinal projections were examined anatomically, such that adult terminal zones would show specific enlargement in the nasotemporal retinal axis. The second is that our anatomical data describe retinal arbors, while our physiological data describe dLGN neurons. Maybe the arbors of adult retinal axons are enlarged in all directions, but dLGN cells sample from a restricted, nasotemporally expanded region within those arbors.

Gain of on/off organization in the $\beta 2^{-/-}$ dLGN is surprising. In respect to this functional attribute, the dLGN of animals that lack retinal waves from P1 to P7 is *more* organized than normal. How could this happen? The model in Figure 6, while containing much conjecture, outlines a possible way in which on/off organization could arise in the $\beta 2^{-/-}$ dLGN. We know that the kind of retinogeniculate information able to segregate on- and off-center inputs, be it spontaneous activity (Wong and Oakley, 1996; Lee et al., 2002) or early, through-the-eyelids visual experience (Akerman et al., 2002), reaches the dLGN rather late. In normal mice, by the time on/off segregating information is available in the thalamus, it may not be able to influence the dLGN's functional organization because the structure is already firmly patterned into ocular laminae (Godement et al., 1984) and probably a coarse retinotopic map, too (Simon and O'Leary, 1992a). In $\beta 2^{-/-}$ mice, though, neither of these patterns has become fully established by the time on/off segregating information might first be available. Mouse vision can begin at P9–P10 (Bonaventure and Karli, 1968; Tian and Copenhagen, 2003), and we know that naturalistic visual experience at this developmental stage can introduce powerful anticorrelations between on- and off-center dLGN cell firing patterns (Akerman et al., 2002). Perhaps because they have more of a "blank slate" to work on in $\beta 2^{-/-}$ mice, these powerful anticorrelations might be able to contribute to functional organization in the dLGN. It would certainly be interesting to see whether altering visual experience or blocking neuronal activity during the second postnatal week in $\beta 2^{-/-}$ mice leads to their on/off "organization" becoming normal again! Alternatively, as well as providing a blank

slate for on/off segregating information to work with, abnormal early spontaneous activity or a lack of thalamic nAChR activity in $\beta 2^{-/-}$ mice might extend or increase plasticity in the retinofugal projections (Grant et al., 1992). This could render late on/off segregating information even more powerful and more likely to pattern the dLGN in $\beta 2^{-/-}$ mice compared to their wt counterparts.

Experimental Procedures

Animals

Wild-type mice were of the C57Bl/6J strain. $\beta 2^{-/-}$ mice, produced at the Pasteur Institute and backcrossed for at least 12 generations onto this strain, have been described previously (Picciotto et al., 1995). All animals were male and were used in accordance with the French Centre National de la Recherche Scientifique guidelines for care and use of laboratory animals (anatomical tracing) or under the auspices of the UK Home Office project and personal licenses held by I.D.T. and M.S.G. (physiological recording).

Anatomical Tracing

Following a previously described protocol (Simon and O'Leary, 1990), approximately 50 nl of a 10% solution of 1,1'-dioctadecyl-3,3,3',3'-tetramethylindocarbocyanineperchlorate (DiI, Molecular Probes, in dimethylformamide, Sigma) was pressure injected into the peripheral nasal or temporal margin of the retina in anesthetized mice (2.5% avertin in PBS at 3 μ l/g i.p.) at postnatal day (P) 12. After 2 days' recovery, P14 mice were deeply anesthetized with 4% chloral hydrate in PBS (10 μ l/g i.p.) and transcardially perfused with PBS (37°C) followed by 4% paraformaldehyde in PBS (4°C).

After overnight post-fixation, the retina was dissected and whole-mounted to analyze the size and location of injection sites. Data were analyzed only from well-localized injections that covered $\leq 1\%$ of the total retinal area. No significant differences in injection size were observed between wt and $\beta 2^{-/-}$ mice (wt mean \pm SEM, 0.69% \pm 0.04% of total retinal area, n = 25; $\beta 2^{-/-}$, 0.72% \pm 0.05% of total retinal area, n = 24; t test, p = 0.61). 200 μ m sections of the brain were cut horizontally on a vibratome, mounted, cover-slipped with Mowiol 4-88 (Calbiochem, CA), and observed with an epifluorescent microscope (Olympus BX51).

Images of the dLGN contralateral to the injected retina were acquired with a CCD video camera (Sony ExwaveHAD) and were used in conjunction with the ImageJ program (<http://rsb.info.nih.gov/ij/>) to quantify terminal zones (TZs) in the most strongly labeled section of each dLGN. TZ areas were obtained by either manually outlining the labeled region or by measuring the image area that exceeded a certain threshold intensity. Both methods produced identical results. TZ optical densities were transformed from mean gray image values following Lambert-Beer's Law.

Physiological Recording

Adult mice (>3 months) were initially anesthetized with 25% Hypnorm (Janssen Animal Health, UK) and 25% Hypnovel (Roche Products Ltd) in water for injections (2.7 μ l/g i.p.) while a tracheotomy was performed and a small plastic tube was inserted. Mice were placed in a stereotaxic apparatus before the tracheal tube was connected to a respiratory pump (MiniVent 845, Hugo Sachs Elektronik, Germany), which supplied a 1:3 mixture of oxygen and nitrous oxide along with 1%–1.5% halothane for maintained anesthesia. Expired CO₂ was monitored (CWE Inc, PA) and maintained at 2.5%–4%, heart rate was monitored with an ECG (~ 5 Hz was normal), and body temperature, measured with a rectal probe, was maintained at $\sim 37^\circ\text{C}$ by combining high ambient temperature with heat from a thermostatically coupled blanket (NP 50-7061-R, Harvard Apparatus). Optics were also continuously monitored for any signs of lens opacity (Fraunfelder and Burns, 1970). Animals were not paralyzed, but measuring eye movements by remapping receptive field locations at intervals of 0.5–1 hr showed positional changes over time to be very small and no different between wt and $\beta 2^{-/-}$ mice (nasotemporal shifts: wt mean \pm SEM, 1.7° \pm 0.5°; $\beta 2^{-/-}$, 2.7° \pm 0.8°; t test with Welch correction, p = 0.3; dorsoventral shifts: wt median,

2.4°; $\beta 2^{-/-}$, 1°; Mann-Whitney test, $p = 0.2$). After a small unilateral craniotomy and durotomy, a tungsten-in-glass recording electrode (Alan Ainsworth, UK) was lowered vertically into the brain. Signals were then filtered and thresholded in order to isolate the responses of single neurons.

Stimulus Presentation

The first visually responsive neuron on each penetration was identified using a hand-held ophthalmoscope. Once the stimulus display (a CRT monitor controlled by a Cambridge Research Systems VSG 2/4 graphics card) had been localized to the appropriate region of visual space for a given penetration, subsequent recorded cells were identified using drifting vertical sinusoidal gratings. These stimuli gave no indication of a cell's RF position within the display, nor whether a cell's responses were on- or off-center. For objective receptive field mapping to provide this information, we presented randomized sequences of white (99 cd/m²) or black (2 cd/m²) square stimuli at various positions on a gray background of mean luminance (48 cd/m²). These stimuli were 10–30 degrees square (depending on viewing distance) and were presented for 200 ms at 192 positions on a 16 × 12 grid. Each square was centered on one grid position but occupied nine of them, such that stimuli were considerably spatially overlapped. Separate on and off RF profiles were constructed by counting the number of spikes elicited when a stimulus of a particular polarity (white for on, black for off) and centered at a particular point on the display, was presented (Jones and Palmer, 1987; Akerman et al., 2002). Locations and polarities that did not elicit a significant response (>2 standard deviations above spontaneous firing, measured to the gray mean luminance background alone) were assigned a count of zero, and then the response at all points was normalized by dividing by the response to the optimal stimulus, regardless of position or polarity. The on and off profiles were subsequently overlaid to construct the overall RF profile. This was smoothed with a Gaussian filter, chosen such that within the distance between two adjacent points of the original profile, the Gaussian decayed to less than 10%. RF locations from these profiles were obtained either by eye or by fitting a two-dimensional Gaussian model to the unsmoothed data. Locations from these two methods were in extremely close agreement in both visual directions (nasotemporal, Pearson $r = 0.997$, $p < 0.0001$; dorsoventral, Pearson $r = 0.988$, $p < 0.0001$).

Localization of Recorded dLGN Cells

At the end of each experiment, animals were perfused transcardially with PBS followed by 4% paraformaldehyde in 0.1 M phosphate buffer. The brain was removed, sunk in 30% sucrose, and sectioned coronally at 30 μ m on a freezing microtome. Staining mounted sections with cresyl violet allowed reconstruction of electrode tracks and the localization of recorded dLGN cells using small (6 μ A for 6 s) electrolytic lesions made during successful penetrations. The angle of electrode tracks relative to the dorsal surface of the dLGN did not differ between wt and $\beta 2^{-/-}$ mice (wt mean \pm SEM, $71^\circ \pm 2^\circ$; $\beta 2^{-/-}$, $69^\circ \pm 2^\circ$; t test, $p = 0.52$). Only cells unequivocally located within the dLGN were included in analyses of functional organization.

Analysis of Functional Organization

RF location separations in visual space (Δ RF(N7) and Δ RF(DV)) were directional measures: if the RF of the cell that was more ventral in the dLGN was more temporal and dorsal than the RF of the cell that was more dorsal in the dLGN, Δ RF(N7) and Δ RF(DV) were *positive*. If the RF of the cell that was more ventral in the dLGN was more ventral and nasal than the RF of the cell that was more dorsal in the dLGN, these distances were *negative*. Plots of cell separation versus RF separation were compared (see Results: Independence of Functional Attributes) using statistical tests for the difference between two correlation coefficients, and for the difference between the slope and intercept of best-fitting linear regressions to the data (Zar, 1984).

Nearest neighbor analysis of on/off organization utilized the following simple binomial model. If on- and off-center cells are arranged randomly in the dLGN, the probability that a nearest neighbor

is of the same center type ($p(\text{same})$) is determined by the relative numbers of on- and off-center cells in a given sample. Specifically:

$$p(\text{same}) = p(\text{on})^2 + p(\text{off})^2$$

Where $p(\text{on})$ is the probability of observing an on-center cell, and $p(\text{off})$ is the probability of observing an off-center cell. This $p(\text{same})$ value can then be used to calculate the expected number of same center-type nearest neighbor pairs in a sample of a given size.

Acknowledgments

The authors would like to thank Darragh Smyth, Louise Upton, Michele Zoli, and Pierre Godement for helpful discussions, Colin Blakemore for temporary laboratory space, and Pierre-Marie Lledo for technical support. M.S.G. is supported by The Wellcome Trust. F.M.R. and J.-P.C. are supported by Collège de France, ARC, and CEE.

Received: July 29, 2003

Revised: October 14, 2003

Accepted: November 24, 2003

Published: December 17, 2003

References

- Akerman, C.J., Smyth, D., and Thompson, I.D. (2002). Visual experience before eye-opening and the development of the retinogeniculate pathway. *Neuron* 36, 869–879.
- Bansal, A., Singer, J.H., Hwang, B.J., Xu, W., Beaudet, A., and Feller, M.B. (2000). Mice lacking specific nicotinic acetylcholine receptor subunits exhibit dramatically altered spontaneous activity patterns and reveal a limited role for retinal waves in forming ON and OFF circuits in the inner retina. *J. Neurosci.* 20, 7672–7681.
- Bonaventure, N., and Karli, P. (1968). Maturation of ERG and evoked visual potentials in mice. *C. R. Seances Soc. Biol. Fil.* 162, 553–555.
- Butts, D.A. (2002). Retinal waves: implications for synaptic learning rules during development. *Neuroscientist* 8, 243–253.
- Chalupa, L.M., and Snider, C.J. (1998). Topographic specificity in the retinocollicular projection of the developing ferret: an anterograde tracing study. *J. Comp. Neurol.* 392, 35–47.
- Chen, C., and Regehr, W.G. (2000). Developmental remodeling of the retinogeniculate synapse. *Neuron* 28, 955–966.
- Edwards, J.A., and Cline, H.T. (1999). Light-induced calcium influx into retinal axons is regulated by presynaptic nicotinic acetylcholine receptor activity in vivo. *J. Neurophysiol.* 81, 895–907.
- Eglen, S.J. (1999). The role of retinal waves and synaptic normalization in retinogeniculate development. *Philos. Trans. R. Soc. Lond. B Biol. Sci.* 354, 497–506.
- Eysel, U.T., Pape, H.C., and Van Schayck, R. (1986). Excitatory and differential disinhibitory actions of acetylcholine in the lateral geniculate nucleus of the cat. *J. Physiol.* 370, 233–254.
- Feldheim, D.A., Vanderhaeghen, P., Hansen, M.J., Frisen, J., Lu, Q., Barbacid, M., and Flanagan, J.G. (1998). Topographic guidance labels in a sensory projection to the forebrain. *Neuron* 21, 1303–1313.
- Feller, M.B., Wellis, D.P., Stellwagen, D., Werblin, F.S., and Shatz, C.J. (1996). Requirement for cholinergic synaptic transmission in the propagation of spontaneous retinal waves. *Science* 272, 1182–1187.
- Francesconi, W., Muller, C.M., and Singer, W. (1988). Cholinergic mechanisms in the reticular control of transmission in the cat lateral geniculate nucleus. *J. Neurophysiol.* 59, 1690–1718.
- Fraunfelder, F.T., and Burns, R.P. (1970). Acute reversible lens opacity: caused by drugs, cold, anoxia, asphyxia, stress, death and dehydration. *Exp. Eye Res.* 10, 19–30.
- Galli, L., and Maffei, L. (1988). Spontaneous impulse activity of rat retinal ganglion cells in prenatal life. *Science* 242, 90–91.
- Godement, P., Salaun, J., and Imbert, M. (1984). Prenatal and postnatal development of retinogeniculate and retinocollicular projections in the mouse. *J. Comp. Neurol.* 230, 552–575.
- Grant, S., Dawes, E.A., and Keating, M.J. (1992). The critical period

- for experience-dependent plasticity in a system of binocular visual connections in *Xenopus laevis*: its extension by dark-rearing. *Eur. J. Neurosci.* 4, 37–45.
- Grubb, M.S., and Thompson, I.D. (2003). Quantitative characterization of visual response properties in the mouse dorsal lateral geniculate nucleus. *J. Neurophysiol.*, in press. Published online August 27, 2003. 10.1152/jn.00699.
- Huberman, A.D., Stellwagen, D., and Chapman, B. (2002). Decoupling eye-specific segregation from lamination in the lateral geniculate nucleus. *J. Neurosci.* 22, 9419–9429.
- Huberman, A.D., Wang, G.Y., Liets, L.C., Collins, O.A., Chapman, B., and Chalupa, L.M. (2003). Eye-specific retinogeniculate segregation independent of normal neuronal activity. *Science* 300, 994–998.
- Jones, J.P., and Palmer, L.A. (1987). The two-dimensional spatial structure of simple receptive fields in cat striate cortex. *J. Neurophysiol.* 58, 1187–1211.
- King, W.M. (1990). Nicotinic depolarization of optic nerve terminals augments synaptic transmission. *Brain Res.* 527, 150–154.
- King, A.J., Schnupp, J.W., and Thompson, I.D. (1998). Signals from the superficial layers of the superior colliculus enable the development of the auditory space map in the deeper layers. *J. Neurosci.* 18, 9394–9408.
- Lee, C.W., Eglén, S.J., and Wong, R.O. (2002). Segregation of ON and OFF retinogeniculate connectivity directed by patterned spontaneous activity. *J. Neurophysiol.* 88, 2311–2321.
- Lena, C., and Changeux, J.P. (1997). Role of Ca²⁺ ions in nicotinic facilitation of GABA release in mouse thalamus. *J. Neurosci.* 17, 576–585.
- McCormick, D.A., and Pape, H.C. (1988). Acetylcholine inhibits identified interneurons in the cat lateral geniculate nucleus. *Nature* 334, 246–248.
- McCormick, D.A., and Prince, D.A. (1987). Actions of acetylcholine in the guinea-pig and cat medial and lateral geniculate nuclei, in vitro. *J. Physiol.* 392, 147–165.
- Meister, M., Wong, R.O., Baylor, D.A., and Schatz, C.J. (1991). Synchronous bursts of action potentials in ganglion cells of the developing mammalian retina. *Science* 252, 939–943.
- Metin, C., Godement, P., Saillour, P., and Imbert, M. (1983). Physiological and anatomical study of the retinogeniculate projections in the mouse. *C. R. Seances Acad. Sci. III* 296, 157–162.
- Muir-Robinson, G., Hwang, B.J., and Feller, M.B. (2002). Retinogeniculate axons undergo eye-specific segregation in the absence of eye-specific layers. *J. Neurosci.* 22, 5259–5264.
- Naeff, B., Schlumpf, M., and Lichtensteiger, W. (1992). Pre- and postnatal development of high-affinity [³H]nicotine binding sites in rat brain regions: an autoradiographic study. *Brain Res. Dev. Brain Res.* 68, 163–174.
- Penn, A.A., Riquelme, P.A., Feller, M.B., and Schatz, C.J. (1998). Competition in retinogeniculate patterning driven by spontaneous activity. *Science* 279, 2108–2112.
- Picciotto, M.R., Zoli, M., Lena, C., Bessis, A., Lallemand, Y., LeNovère, N., Vincent, P., Pich, E.M., Brulet, P., and Changeux, J.P. (1995). Abnormal avoidance learning in mice lacking functional high-affinity nicotine receptor in the brain. *Nature* 374, 65–67.
- Picciotto, M.R., Zoli, M., Rimondini, R., Lena, C., Marubio, L.M., Pich, E.M., Fuxe, K., and Changeux, J.P. (1998). Acetylcholine receptors containing the beta2 subunit are involved in the reinforcing properties of nicotine. *Nature* 397, 173–177.
- Prusky, G.T., and Cynader, M.S. (1988). [³H]nicotine binding sites are associated with mammalian optic nerve terminals. *Vis. Neurosci.* 1, 245–248.
- Rossi, F.M., Pizzorusso, T., Porciatti, V., Marubio, L.M., Maffei, L., and Changeux, J.P. (2001). Requirement of the nicotinic acetylcholine receptor beta 2 subunit for the anatomical and functional development of the visual system. *Proc. Natl. Acad. Sci. USA* 98, 6453–6458.
- Sherman, S.M., and Guillery, R.W. (2002). The role of the thalamus in the flow of information to the cortex. *Philos. Trans. R. Soc. Lond. B Biol. Sci.* 357, 1695–1708.
- Sillito, A.M., Kemp, J.A., and Berardi, N. (1983). The cholinergic influence on the function of the cat dorsal lateral geniculate nucleus (dLGN). *Brain Res.* 280, 299–307.
- Simon, D.K., and O'Leary, D.D. (1990). Limited topographic specificity in the targeting and branching of mammalian retinal axons. *Dev. Biol.* 137, 125–134.
- Simon, D.K., and O'Leary, D.D. (1991). Relationship of retinotopic ordering of axons in the optic pathway to the formation of visual maps in central targets. *J. Comp. Neurol.* 307, 393–404.
- Simon, D.K., and O'Leary, D.D. (1992a). Development of topographic order in the mammalian retinocollicular projection. *J. Neurosci.* 12, 1212–1232.
- Simon, D.K., and O'Leary, D.D. (1992b). Influence of position along the medial-lateral axis of the superior colliculus on the topographic targeting and survival of retinal axons. *Brain Res. Dev. Brain Res.* 69, 167–172.
- Simon, D.K., Prusky, G.T., O'Leary, D.D., and Constantine Paton, M. (1992). N-methyl-D-aspartate receptor antagonists disrupt the formation of a mammalian neural map. *Proc. Natl. Acad. Sci. USA* 89, 10593–10597.
- Stryker, M.P., and Zahs, K.R. (1983). On and off sublaminae in the lateral geniculate nucleus of the ferret. *J. Neurosci.* 3, 1943–1951.
- Swanson, L.W., Simmons, D.M., Whiting, P.J., and Lindstrom, J. (1987). Immunohistochemical localization of neuronal nicotinic receptors in the rodent central nervous system. *J. Neurosci.* 7, 3334–3342.
- Tian, N., and Copenhagen, D.R. (2003). Visual stimulation is required for refinement of ON and OFF pathways in postnatal retina. *Neuron* 39, 85–96.
- Wagner, E., McCaffery, P., and Drager, U.C. (2000). Retinoic acid in the formation of the dorsoventral retina and its central projections. *Dev. Biol.* 222, 460–470.
- Wong, R.O., and Oakley, D.M. (1996). Changing patterns of spontaneous bursting activity of on and off retinal ganglion cells during development. *Neuron* 16, 1087–1095.
- Wong, W.T., Myhr, K.L., Miller, E.D., and Wong, R.O. (2000). Developmental changes in the neurotransmitter regulation of correlated spontaneous retinal activity. *J. Neurosci.* 20, 351–360.
- Yu, C.J., Butt, C.M., and Debski, E.A. (2003). Bidirectional modulation of visual plasticity by cholinergic receptor subtypes in the frog optic tectum. *Eur. J. Neurosci.* 17, 1253–1265.
- Zar, J.H. (1984). *Biostatistical Analysis*, Second Edition (Englewood Cliffs: Prentice-Hall).
- Zhu, J.J., and Uhlrich, D.J. (1997). Nicotinic receptor-mediated responses in relay cells and interneurons in the rat lateral geniculate nucleus. *Neuroscience* 80, 191–202.
- Zoli, M., Lena, C., Picciotto, M.R., and Changeux, J.P. (1998). Identification of four classes of brain nicotinic receptors using beta2 mutant mice. *J. Neurosci.* 18, 4461–4472.